Journal of Non-Crystalline Solids 354 (2008) 3785–3792

Contents lists available at ScienceDirect

Journal of Non-Crystalline Solids

journal homepage: www.elsevier.com/locate/jnoncrysol

# Nucleation time-lag from nucleation and growth experiments in deeply undercooled glass-forming liquids

Vladimir M. Fokin [a,*], Nikolay S. Yuritsyn [b], Edgar D. Zanotto [c], Jürn W.P. Schmelzer [d], Aluisio A. Cabral [e]

[a] Vavilov State Optical Institute, ul. Babushkina 36-1, 193171 St. Petersburg, Russia
[b] Grebenshchikov Institute of Silicate Chemistry, Russian Academy of Sciences, ul. Odoevskogo 24-2, 199155 St. Petersburg, Russia
[c] LaMaV – Vitreous Materials Laboratory, Federal University of São Carlos, 13565-905 São Carlos, SP, Brazil
[d] Institut für Physik, Universität Rostock, 18051 Rostock, Germany
[e] Department of Exact Sciences, Federal Center for Technological Education, 65025-001 São Luis, MA, Brazil

ARTICLE INFO

*Article history:*
Received 6 December 2007
Received in revised form 7 May 2008
Available online 21 June 2008

*PACS:*
81.10.Aj
64.60.Q
72.80.Ng
64.70.dg

*Keywords:*
Crystal growth
Nucleation
Alkali silicates
Soda–lime–silica

ABSTRACT

A new approach is proposed to explain the strong difference between the induction periods (nucleation time-lags) obtained from nucleation rate measurements and from crystal growth experiments for lithium silicate glasses; and their similar magnitude for a $Na_2O \cdot 2CaO \cdot 3SiO_2$ glass. For these two glass families, the time-lags for nucleation estimated from crystal growth kinetics were compared with those directly obtained from nucleation experiments. A theoretical analysis was performed employing analytical solutions of the Frenkel–Zeldovich equation. In such analysis, the frequently assumed condition of size-independence of the thermodynamic properties of the crystallites was used. Provided this assumption is correct, time-lag data obtained in the two above mentioned ways should coincide. Consequently the significant difference between the values of nucleation time-lag for lithium silicate glasses from nucleation and growth data gives a strong indirect evidence for the deviation of the properties of critical nuclei from the respective parameters characterizing the state of the newly evolving macrophase. For $Na_2O \cdot 2CaO \cdot 3SiO_2$ glass at intermediate stages of crystallization we show that the average composition of the growing crystals is close to that of the near-critical nuclei. The fact that the nucleation and growth rates of this soda–lime–silica glass refer to the same phase provides an explanation for the similarity of the induction periods estimated from nucleation and growth experiments.

© 2008 Elsevier B.V. All rights reserved.

## 1. Introduction

A key problem in the application of nucleation theories for the analysis of nucleation kinetics in undercooled liquids is the correct choice of the properties of the critical nuclei. However, quantitative information about the critical nuclei in condensed systems is rarely available due to their extremely small size at the deep undercoolings that are typically needed to attain measurable nucleation rates.

In the framework of the classical nucleation theory (CNT), which is commonly used for the analysis of crystal nucleation in glass-forming liquids, the thermodynamic properties of the aggregates of the evolving new phase are considered to be size-independent [1]. This assumption allows one to identify the properties of the (nanosized) critical clusters with those of the evolving macroscopic phases. As a result, a qualitatively correct description of the time and temperature dependencies of the nucleation rates is typically obtained. However, in a variety of cases this assumption leads to drastic discrepancies between the magnitudes of calculated and measured nucleation rates; i.e. the nucleation rates are underestimated by 10–100 orders of magnitude [2]. These discrepancies and other theoretical and experimental evidence lead to severe doubts concerning the correctness of the main assumption of CNT, i.e. that the critical clusters and the respective macroscopic phase are characterized by the same bulk and surface properties [3]. Some examples of such evidences will be discussed latter in this article.

Analyzes of the nucleation kinetics in undercooled liquids can be supplemented by independent measurements of crystal growth rates in the same temperature range, since growth is a fundamental part of the general nucleation-growth-crystallization process. Fifteen years ago an interesting finding was reported in a study of nucleation-growth processes in lithium disilicate glass [4]. This glass has been used for a long time as a model system for nucleation studies, so those findings are of general relevance. In the mentioned study [4], the induction periods for growth, $t^g_{ind}$, and nucleation, $t^n_{ind}$, were compared. The values of these characteristic times are commonly determined in a way illustrated in Fig. 1, based on newly performed measurements, via the intersections

* Corresponding author. Tel.: +7 812 355 30 38.
*E-mail address:* vfokin@pisem.net (V.M. Fokin).

0022-3093/$ - see front matter © 2008 Elsevier B.V. All rights reserved.
doi:10.1016/j.jnoncrysol.2008.05.011

with the time axis of linear fits of the $N(t)$ and $R(t)$-dependencies, where $N(t)$ is the crystal number density and $R(t)$ is the size (radius) of the largest crystals. In Ref. [4] it was shown that the experimentally determined induction periods for growth, $t^g_{ind}$, noticeably exceed the values $t^n_{ind}$ obtained from nucleation data.

To a first approximation, the induction period for growth can be represented as the sum of two characteristic times: the time needed for the formation of a sufficient number of critical nuclei allowing one to detect them at the advanced stage of growth (this time is close to $t^n_{ind}$, which is connected with the time-lag for nucleation by a numerical factor, as will be shown later) plus the time required to arrive at a constant (size-independent) crystal growth rate.

The time-lag for nucleation is a measure of the time required to establish steady-state conditions in the range of sub-critical cluster sizes. Hence, if one neglects the time for establishment of a constant growth rate in comparison with the time-lag for nucleation, then $t^g_{ind}$ and $t^n_{ind}$ must have similar magnitudes [5], provided crystal nucleation and macroscopic growth refer to the formation of the same phase. However, as above mentioned, some experiments with Li-silicate glasses did not confirm such expectations. In order to reconcile this discrepancy, an attempt was undertaken in Ref. [4] to account for the effect of a size-dependent growth rate for the correction of the value of $t^g_{ind}$. However, even accounting for such effects, the difference between $t^g_{ind}$ and $t^n_{ind}$ for lithium disilicate remained too high.

In contrast to lithium disilicate glass, the induction periods for nucleation and growth in two soda–lime–silica glasses ($Na_2O \cdot 2CaO \cdot 3SiO_2$ ($N_1C_2S_3$) and $2Na_2O \cdot CaO \cdot 3SiO_2$ ($N_2C_1S_3$)) have similar magnitudes, in line with the above mentioned expectations [4]. From these results it was concluded in Ref. [4] that in the case of these soda–lime–silica glasses the classical assumption describes the situation correctly, while for lithium disilicate a metastable phase, which precipitates in the early stage of crystallization, acts as a precursor of crystallization of the finally evolving macroscopic phase. That is, in order to explain the above mentioned deviations of experimental data and theoretical expectations, differences in the bulk properties of nucleating and growing crystals were assumed.

However, in Ref. [4], the crystal growth rates were determined by single-stage heat treatment, while the crystal nucleation rates were determined by double-stage heat treatment (the so-called 'development' method [3], i.e. first treated at the nucleation temperature and then at a higher temperature for growth). In Ref. [6] measurements of crystal nucleation and growth rates and of the corresponding induction periods in lithium disilicate glass were carried out using both single-stage (ST) and double-stage (DT) heat treatments at a relatively high temperature, 500 °C > $T_{max}$ = 455 °C ($T_{max}$ is the temperature of the nucleation rate maximum). The estimated (extrapolated) induction period for nucleation from ST was considerably higher than that obtained by the 'development' method and practically agreed with the induction period for crystal growth. However, it was shown later [3] that this result was due to an insufficient account of stereological corrections of the crystal number density in the samples subjected to single-stage treatments. When proper mathematical corrections are made for the number of crystals with sizes below the resolution limit of the optical microscope in single-stage treatments, the induction period for nucleation estimated by single and double-stage treatments almost coincide, and are significantly smaller than that for crystal growth.

In the present paper we reconsider this problem by extending crystal growth rate measurements down to the temperature range of maximum nucleation rates (close to the glass transition temperature $T_g$), and the compositional range of lithium silicate glasses from 32 to 37 mol% $Li_2O$. We then analyze the results using a different approach from that of Refs. [4,6], because we do not consider the induction period for growth, but instead the time-lag for nucleation estimated from crystal growth kinetics employing analytical solutions of the Frenkel–Zeldovich equation, which give a correct description of the cluster size evolution. In other words, we do not use any macroscopic growth equation *per se*. Thus, we avoid here the procedure employed in Refs. [4,6] where macroscopic growth equations were used to describe cluster growth, starting from critical sizes, to account for the size effect on the growth rate. Since the growth rate of the critical clusters is null, the numerical integration performed in Refs. [4,6] is very sensitive to the lower limit of integration chosen, and thus could not properly correct $t^g_{ind}$. In addition, in analyzing the new nucleation and growth data for $N_1C_2S_3$ glass, we also account for the evolution of the crystal composition in this particular glass, which was not known when Ref. [4] was published.

The objective of this paper is thus to employ a new approach to an old problem using new information about the crystallization pathways and extensive new measurements of crystal growth kinetics.

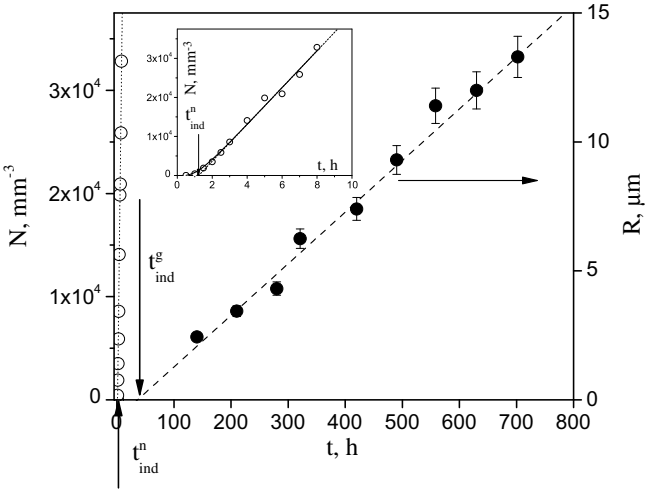


**Fig. 1.** Crystal number density, $N$, estimated by the 'development' method and size of the largest crystals, $R$, in glass L3 versus heat treatment time at $T$ = 458 °C. The dashed line is a linear approximation to $R(t)$-data. The solid and dotted lines were plotted via Eqs. (2) and (3), respectively.

## 2. Equations employed for the analysis of nucleation and growth kinetics

### 2.1. Nucleation kinetics

According to Collins and Kashchiev [7,8], the non steady-state nucleation rate can be written as

$$I(t) = I_{st}\left[1 + 2\sum_{m=1}^{\infty}(-1)^m \exp\left(-m^2\frac{t}{\tau_{C\&K}}\right)\right], \quad (1)$$

where $I_{st}$ is steady-state nucleation rate of critical size clusters, $t$ is time, and $\tau_{C\&K}$ is the time-lag for nucleation (a characteristic time scale required to establish steady-state conditions for clusters up to critical sizes). Integration of Eq. (1) results in the following expression for the time-dependence of the number of super-critical nuclei per unit volume, $N_V$,

$$\frac{N_V(t)}{I_{st}\tau_{C\&K}} = \left[\frac{t}{\tau_{C\&K}} - \frac{\pi^2}{6} - 2\sum_{m=1}^{\infty}\frac{(-1)^m}{m^2}\exp\left(-m^2\frac{t}{\tau_{C\&K}}\right)\right]. \quad (2)$$

For sufficiently long times, $t \gg \tau_{C\&K}$, this expression can be approximated by

$$N_V(t) = I_{st}\left(t - \frac{\pi^2}{6}\tau_{C\&K}\right). \quad (3)$$

For the experimental estimation of $\tau_{C\&K}$, the induction period for nucleation, $t^n_{ind}$, defined via Eq. (4)

$$t^n_{ind} = \frac{\pi^2}{6}\tau_{C\&K}, \quad (4)$$

is frequently used. A more correct way to estimate the steady-state nucleation rate and the time-lag for nucleation is by fitting experimental $N_V(t)$ data via Eq. (2) using $I_{st}$ and $\tau_{C\&K}$ as adjustable parameters.

In our analysis, we use the following equation to estimate the thermodynamic barrier $W_*$ for homogeneous volume nucleation via experimental steady-state nucleation rate [1]

$$I_{st} = \frac{16}{3}\frac{(k_B T)^{1/2}}{l^6}\frac{\sigma^{3/2}}{\Delta G_V^2 t^n_{ind}}\exp\left(-\frac{W_*}{k_B T}\right), \quad (5)$$

where $k_B$ is Boltzmann's constant, $l$ the mean size of the structural (formula) units, $\sigma$ the specific surface free energy of the critical nucleus/melt interface, $t^n_{ind}$ the induction period for nucleation (see Eq. (4)), and $\Delta G_V$ the difference between the free energies of liquid and crystal per unit volume of crystal, i.e. the thermodynamic driving force for crystallization. Employing, in addition the following approximation, usually assigned to Turnbull,

$$\Delta G_V = \Delta H_V\left(1 - \frac{T}{T_{m/L}}\right), \quad (6)$$

where $\Delta H_V$ is the melting enthalpy per unit volume of crystal and $T_{m/L}$ is the melting or liquidus temperature, Eq. (5) can be rewritten as

$$\frac{W_*}{k_B T} = \ln\left[\frac{16 k_B^{1/2}}{3}\frac{\sigma^{3/2}}{\Delta H_V^2 l^6}\right] - \ln\left[I_{st} t^n_{ind}\frac{(T_{m/L} - T)^2}{T^{1/2} T^2_{m/L}}\right]. \quad (7)$$

Eq. (7) will be used to estimate $W_*$ required to employ Shneidman's solution of the Frenkel–Zeldovich equation (see next section).

### 2.2. Crystal growth kinetics

In the analysis of experimental data on the growth kinetics of near-critical clusters, we use here two other analytical solutions of the Frenkel–Zeldovich equation (that describes nucleation-growth processes) developed by Shneidman [9,10] and Slezov–Schmelzer [11,12] for homogeneous volume nucleation. These two equations can be employed to estimate the time-lag for nucleation using experimental data on crystal growth at deep undercoolings (around $T_g$) for which the nucleation kinetics was also measured. At a first glance, the scheme of time-lag estimation for nucleation-growth processes from experimental $N(t)$-curves proposed by Shneidman [10] seems to be quite straightforward. However, the selection of the linear part of the $N(t)$-curve needed to estimate the steady-state nucleation rate, $I_{st}$, and induction period, $t^n_{ind}$, is a subjective procedure considering that any $N(t)$-curve asymptotically approaches a linear dependence. The second problem refers to the estimation of $N(t^n_{ind})$. The issue here is that the most reliable measurements refer, as a rule, only to times larger than $t^n_{ind}$, moreover, data for $t \sim t^n_{ind}$ are sometimes absent. The above mentioned features lead to the common use of the Collins–Kashchiev solution, which allows one to obtain the steady-state nucleation rate and time-lag for nucleation as fit parameters by fitting all experimental $N(t)$-data. This approach works even if only $N(t)$-data are available which are far from steady-state conditions.

#### 2.2.1. Slezov–Schmelzer's solution

According to Refs. [11,12], at $R \geqslant 2R_*$ where $R_*$ is the critical size, the radius of the largest observable nuclei is connected with time via

$$\hat{\tau} = \frac{32}{20}\left\{1 + \frac{3}{4}\left[\frac{\hat{R}}{2} - 1\right]\right\} \quad (8)$$

or

$$\hat{R} = \frac{5}{3}\hat{\tau} - \frac{2}{3}, \quad (9)$$

where the dimensionless variables

$$\hat{R} \equiv \frac{R}{R_*},\ \hat{\tau} \equiv \frac{t}{\tau_{S\&S}} \quad (10)$$

are employed. In these derivations it was assumed that: (i) the bulk properties of the clusters are size-independent and are thus equal to those of the newly evolving macrophase; (ii) the growth mechanism does not depend on cluster size and (iii) growth is kinetically limited.

These assumptions are commonly employed in CNT. The growth rate can be derived from Eq. (9) to give

$$\frac{d\hat{R}}{d\hat{\tau}} = \frac{5}{3}. \quad (11)$$

If the size-dependence of the crystal growth rate is taken into account via

$$\frac{d\hat{R}}{d\hat{\tau}} = \frac{5}{3}\left(1 - \frac{1}{\hat{R}}\right) \quad (12)$$

one gets the solution

$$\hat{\tau} = \frac{3}{5}\left[\hat{R} + \ln(\hat{R} - 1) + \frac{2}{3}\right]. \quad (13)$$

For large times (and, consequently, large crystal sizes) this result is equivalent to Eq. (9). Recall that the above given equations are valid for $\hat{R} \geqslant 2$.

#### 2.2.2. Shneidman's solution

Shneidman [9,10] proceeded in the analysis of the Frenkel–Zeldovich equation differently from Slezov and Schmelzer [11,12]. The structure of his resulting equation for the size-dependent time-lag, $\hat{\tau}$, is, however, widely equivalent and is given by

$$\hat{\tau} = \hat{R} + \ln(\hat{R} - 1) + \ln\frac{6W_*}{k_B T} - 2 + \gamma, \quad (14)$$

where $\gamma$ is Euler's constant ($\gamma = 0.57721$), $\hat{R}$ and $\hat{\tau}$ are dimensionless variables as in Eqs.(8)–(13).

One should note that, if compared with Eqs. (13) and (14) additionally includes the thermodynamic barrier for nucleation, $W_*$. This fact was employed in Ref. [13] to estimate the surface energy of the critical nucleus/melt interface for lithium disilicate glass using the time needed for the clusters to reach a given crystal size. As for Eq. (13), Eq. (14) was derived on the assumption that the bulk properties of the clusters do not depend on their size, and that growth is kinetically limited. Note, moreover, that the nucleation time-lags in the solutions of Slezov & Schmelzer, $\tau_{S\&S}$, Shneidman, $\tau_S$, and Collins & Kashchiev, $\tau_{C\&K}$, correspond to different moments of the phase transition process. The following approximate relations between these time-lags hold [8–12]

$$\tau_{S\&S} \approx 5\tau_{C\&K}, \quad (15)$$

$$\tau_S = \frac{\pi^2}{8}\tau_{C\&K} \approx 1.23\tau_{C\&K}. \quad (16)$$

In this article we employ all these equations to compare the values of time-lags estimated from nucleation ($\tau_{C\&K}$) and growth ($\tau_{S\&S}$, $\tau_S$) kinetics.

## 3. Systems investigated and methods

Lithium silicate glasses with compositions from 32 to 37 mol% $Li_2O$, belonging to the composition range of solid solution formation, and a sodium–calcium–metasilicate glass with a composition close to stoichiometric $N_1C_2S_3$ were synthesized from lithium, sodium, and calcium carbonates and amorphous silicon dioxide of analytical grate. Their compositions by analysis are presented in Table 1. Optical microscopes (Leica DMRX, Neophot 32, Jenaval) were employed to estimate the crystal size and their number density. Thermal analysis was performed by a ATA Q10 DSC with cooling and heating rates of 10 °C/min.

## 4. Results

### 4.1. Lithium silicate glasses

Figs. 1 and 2 illustrate the evolution of crystal number density, $N$, and size of the largest crystals, $R$, at a temperature close to the maximum of the steady-state nucleation rate in glasses L3 and L1, respectively (cf. Table 1). The induction times for crystal growth, $t^g_{ind}$, estimated from the $R \sim t$ plot (as shown by Figs. 1 and 2) by far exceed the induction times for nucleation, $t^n_{ind}$, estimated by fitting of $N \sim t$ data to Eq. (2). Since the values of $N$ were estimated via the 'development' method, $t^n_{ind}$ is somewhat overestimated as compared with the true value corresponding to the nucleation temperature (this is due to the dissolution of nuclei with sizes in the range between the values of the critical sizes corresponding to nucleation and development temperatures [14]). Thus, the experimentally obtained ratio $t^g_{ind}/t^n_{ind}$ only gives a lower bound for the difference between the real induction periods. Fig. 3 shows that this difference is observed for several temperatures. The closed and open circles refer to glass L1 and data from Ref. [4], respectively. The data for glass L1 further extend the $t^g_{ind}$ versus $T$-plot down to the temperature of nucleation rate maximum, probing one order of magnitude larger $t^g_{ind}$ if compared to the results of Ref. [4].

The experimental $R(t)$-data, such as those shown by Figs. 1 and 2, were fitted to Eqs. (13) and (14) using $\tau_{S\&S}$, $\tau_S$ and $R_*$ as fitting parameters. In the case of Eq. (14), we used the values of the thermodynamic barrier estimated from nucleation data ($I_{st}$ and $t^n_{ind}$) by means of Eq. (7). Table 2 presents the thermodynamic barrier for nucleation in several lithium silicate glasses at $T = 460$ °C, which is close to the temperatures of the nucleation rate maximum. The result of $W_*$ estimation depends on the choice of $\sigma$ and $\Delta G_v$ only weakly. Moreover, the final result is not sensitive to the value of $W_*$. Fig. 4 shows the $R(t)$-data and the result of the fitting procedure. The coordinates of the closed and open stars correspond to the time-lags for nucleation and critical sizes estimated by fitting $R(t)$-data to Eq. (13) and Eq. (14), respectively. A similar procedure was used for glasses L2-L5.

Fig. 5 shows a collection of nucleation time-lags estimated from nucleation (1) and growth kinetics via Eq. (13) (2) and Eq. (14) (3) for several glass compositions at $T = 460$ °C. This temperature is close to the temperatures of nucleation rate maxima. The solid lines are linear approximations. Short-dotted and dashed-dotted lines show the nucleation time-lags calculated from the S&S and S models (see Eqs. (15) and (16)). One should note that the values of $\tau_{C\&K}$ were estimated from fitting $N(t)$-data to Eq. (2). As we already emphasized, an appropriate correction of the $N(t)$-curve and hence of $\tau_{C\&K}$ due to the dissolution of sub-critical nuclei at

**Table 1**
Glass compositions in mol% by analysis

| Glass | $Li_2O$ | $Na_2O$ | CaO | $SiO_2$ |
|---|---|---|---|---|
| L1 | 32.6 | | | 67.4 |
| L2 | 34.3 | | | 65.7 |
| L3 | 35.1 | | | 64.9 |
| L4 | 36.2 | | | 63.8 |
| L5 | 36.7 | | | 63.3 |
| L6 | 37.1 | | | 62.9 |
| $N_1C_2S_3$ | | 17.2 | 32.3 | 50.5 |

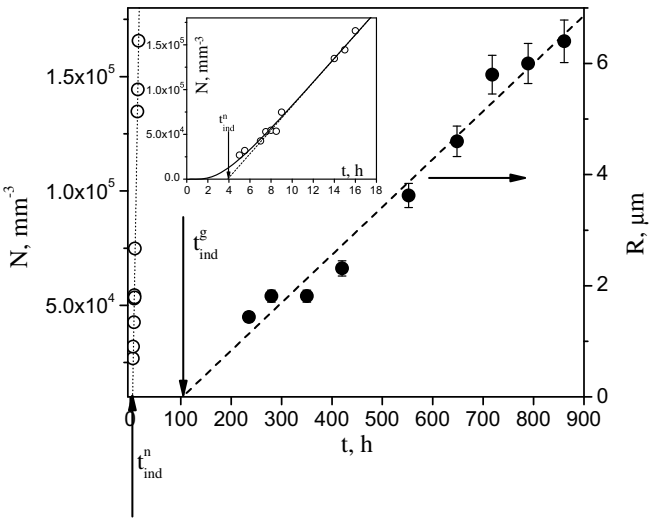


**Fig. 2.** Crystal number density, $N$, estimated by the 'development' method and size of the largest crystals, $R$, in glass L1 versus heat treatment time at $T = 458$ °C. The dashed line is a linear approximation to $R(t)$-data. The solid and dotted lines were plotted via Eqs. (2) and (3), respectively.

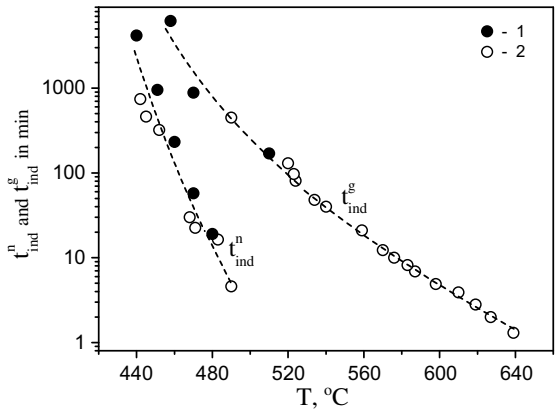


**Fig. 3.** Induction periods for nucleation, $t^n_{ind}$, and for crystal growth, $t^g_{ind}$, versus temperature for lithium silicate glasses. (1) Glass L1 and (2) 33.5 mol% $Li_2O$ [4].

**Table 2**
The thermodynamic barrier for nucleation at $T = 460$ °C for several lithium silicate glasses

| Glass | $W_*$, J |
|---|---|
| L1 | 3.60E−19 |
| L2 | 3.82E−19 |
| L3 | 3.85E−19 |
| L4 | 3.69E−19 |
| L5 | 3.52E−19 |

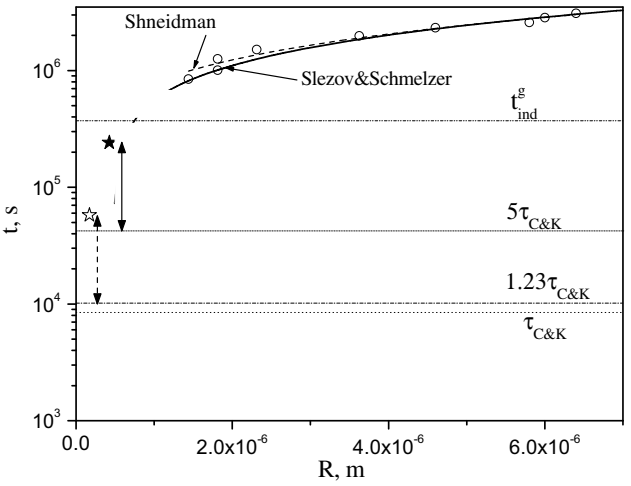


**Fig. 4.** Time $t$ needed to arrive at crystal size $R$ for glass L1 at $T = 458$ °C. The circles refer to experimental data. The solid and dashed lines were plotted by Eqs. (13) and (14), respectively, using $\tau_{S\&S}$ ($\tau_S$) and $R_*$ as fit parameters. The coordinates of the closed and open stars show these parameters estimated via Eqs. (13) and (14), respectively. The dotted, dashed-dotted, and short dotted lines show the values of $\tau_{C\&K}$ (estimated by fit of the $N(t)$ data to Eq. (2)), $1.23\tau_{C\&K}$, and $5\tau_{C\&K}$, respectively. The dashed–dotted–dotted line shows the induction time for growth.

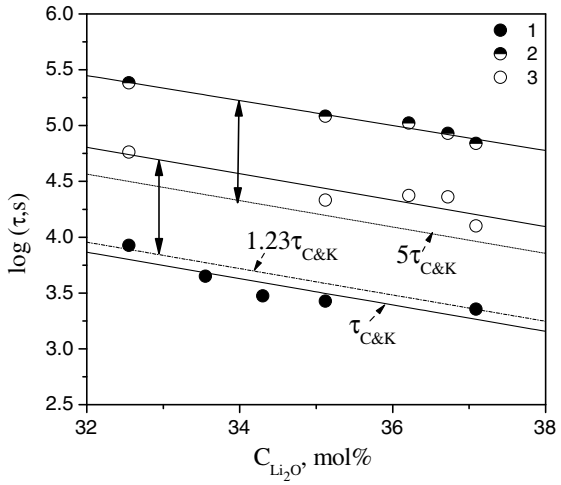


**Fig. 5.** Time-lag for nucleation estimated from $N(t)$ data (1), from growth kinetics via Eq. (13) (2) and Eq. (14) (3) for lithium oxide glasses versus lithium oxide content. The solid lines are linear approximations.

the development temperature [14] would increase the observed difference between the time-lags estimated from growth and nucleation kinetics.

### 4.2. Sodium calcium metasilicate glass

Nucleation and growth kinetics were measured for sodium calcium metasilicate glass at three temperatures close to the temperature of maximum nucleation rate. Figs. 6–8 show the evolution of the crystal number density, $N$, and the size of the largest crystals, $a$, at these temperatures, while Fig. 9 shows measured and literature data for the steady-state nucleation rate in $N_1C_2S_3$ glass. Solid and dashed lines in Figs. 6–8 were plotted by Eqs. (2) and (3), respectively, with $I_{st}$ and $\tau_{C\&K}$ estimated as fitting parameters. The use of relatively low temperatures (lower than that of the nucleation rate maximum, see Fig. 9) allows us to sample longer $t^n_{ind}$ and $t^g_{ind}$, which gives an increased accuracy in their measurement.

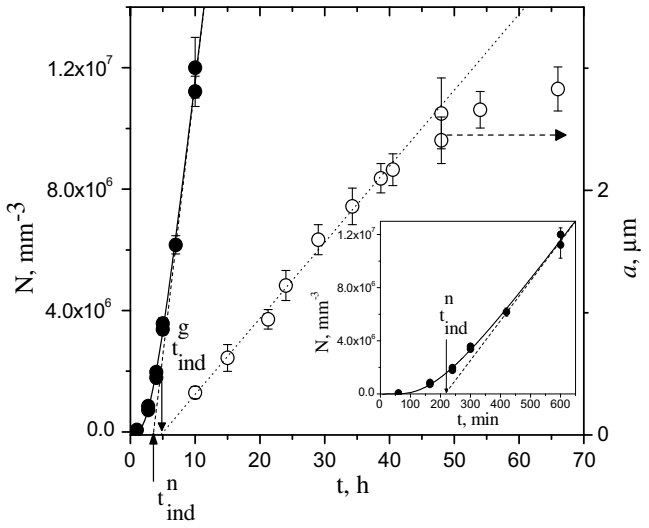


**Fig. 6.** Crystal number density, $N$, and the size of the largest crystals, $a$, versus time of treatment at $T = 580$ °C. The solid lines are plotted by Eq. (2). The dashed line shows their asymptote. The dotted line is a linear fit of the initial part of the $a(t)$-dependence.

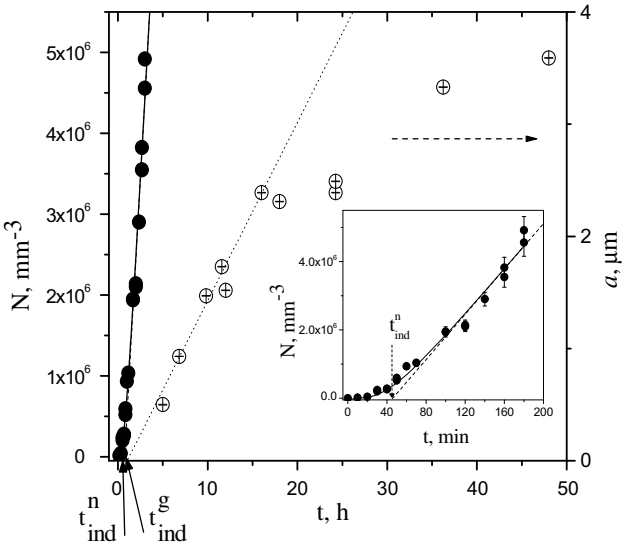


**Fig. 7.** Crystal number density, $N$, and the size of the largest crystals, $a$, versus time of treatment at $T = 590$ °C. The solid lines are plotted by Eq. (2). The dashed line presents their asymptote. The dotted line is a linear fit of the initial part of the $a(t)$-dependence.

## 5. Discussion

### 5.1. Lithium silicate glasses

Figs. 1–3 demonstrate a strong difference between $t^n_{ind}$ and $t^g_{ind}$ corroborating the results of Ref. [4] and extending the measurements of growth kinetics to the temperature of the maximum nucleation rate. However, as we already mentioned, we will not analyze $t^g_{ind}$ and hence will not use any macroscopic growth equation (which is not valid for clusters of critical size) to correct $t^g_{ind}$, as it was performed in Refs. [4,6], but rely instead on analytical solutions of the Zeldovich–Frenkel equation. That is, in this article we fit the experimental $R(t)$-data to Eq. (13) or (14) using $R_*$ and $\tau_{S\&S}$ or $\tau_S$, respectively, as adjustable parameters. As follows from Fig. 4, the values of $\tau_{S\&S}$ and $\tau_S$ denoted by closed and open stars,

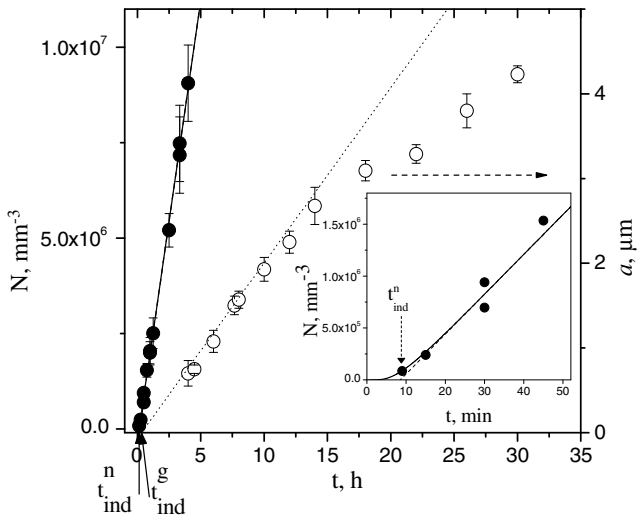


**Fig. 8.** Crystal number density, $N$, and size of the largest crystals, $a$, versus time of heat treatment at $T = 600$ °C. The solid lines are plotted by Eq. (2). The dashed line presents their asymptote. The dotted line is a linear fit of the initial part of the $a(t)$-dependence.

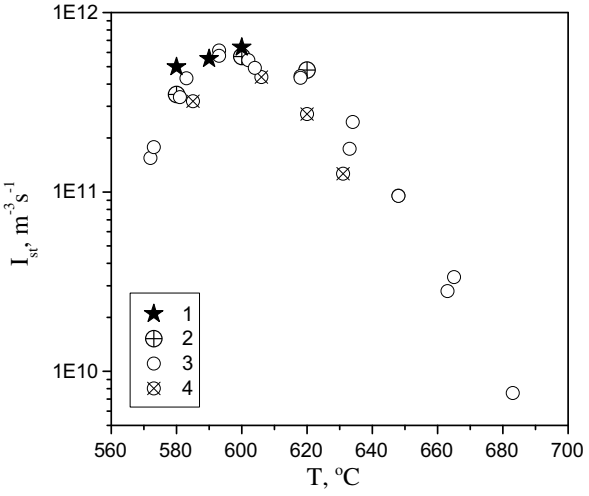


**Fig. 9.** Steady-state nucleation rate in glasses of compositions close to the stoichiometric $Na_2O \cdot 2CaO \cdot 3SiO_2$ *versus* temperature. (1) Present study, (2) [4], (3) [15] and (4) [16].

respectively, considerably exceed the values directly estimated from an $N(t)$-plot via Eq. (2) by Eqs. (15) and (16), marked by short-dotted and dashed-dotted lines, respectively. Vertical lines with arrows show the difference between the values of nucleation time-lags estimated via Eqs. (13) and (14) and those directly evaluated from nucleation $N(t)$-plot. Similar differences were obtained for glasses with compositions within the range of solid solution formation, see Fig. 5. It should be emphasized that for these glasses the crystal growth rates refer to solid solutions having the compositions of their respective parent glasses, resembling a case of stoichiometric crystallization. The use of the 'development' method to obtain $N(t)$-plots results in some overestimation of $\tau_{C\&K}$. Thus, for lithium silicate glasses, the values of $\tau_{S\&S}$ and $\tau_S$ exceed the values calculated by Eqs. (15) and (16), respectively, by a factor not less than 7–8, see Figs. 4 and 5. Since both $\tau_{S\&S}$ ($\tau_S$) and $\tau_{C\&K}$ refer directly to nucleation kinetics, one expects that $\tau_{S\&S} \approx 5\tau_{C\&K}$ and $\tau_S \approx 1.23\tau_{C\&K}$ if the conditions (i)–(iii) (see section 2.2) were fulfilled. Hence the observed discrepancy leads us to the following conclusion: at least one or several of the conditions underlying the derivations of Eqs. (13) and (14) is not valid.

It is reasonable to suppose that the compositions of near-critical clusters deviate, in general, from the composition of the respective macroscopic phase. In this case, diffusion-limited growth of near-critical clusters could take place, while the compositions of the macroscopic phases (lithium disilicate or a solid solution) are equal to those of their parent glasses, and their growth is kinetically limited. However, according to Ref. [17] kinetically limited growth can be expected for small clusters independent on their composition, since transport of matter over long distances is not required to sustain the aggregation process (because a sufficient amount of each component is available in the immediate vicinity of the clusters). Anyway, as shown in Ref. [18], the size-dependence of the cluster composition leads to a size dependence of thermodynamic and kinetic parameters, in particular, the thermodynamic driving force for crystallization.

Moreover, we can conclude that the thermodynamic driving force for nucleation in the considered glasses is smaller than that for growth of the respective macrophase, since the latter is the stable phase having the highest thermodynamic driving force, and any deviation in composition must reduce it. This conclusion corroborates our recent findings based on the comparison of the effective diffusion coefficients controlling nucleation and growth kinetics [19]. The precise way how the properties of the nuclei (e.g. composition) evolve with their size and approach finally the values corresponding to the stable phase is a not trivial and still open question. In the advanced stages of phase transformation, only the stable lithium disilicate or the respective solid solutions were experimentally observed. Here it should be recalled that, e.g., the compositional evolution of the primary phase in a NiP-alloy is almost completed when the size of the nuclei reaches about 8 nm [20], i.e. at sizes, which cannot be studied by most common methods.

### 5.2. $Na_2O \cdot 2CaO \cdot 3SiO_2$ glass

In contrast to lithium silicate glasses, the values of $t^g_{ind}$ for $N_1C_2S_3$ glass only slightly exceed $t^n_{ind}$, see Figs. 6–8. At first sight, this result can be interpreted as evidence that the critical nuclei have the same bulk properties as the stable phase. This explanation was indeed advanced in Ref. [4]. However, as we have shown in Ref. [22], the formation of $Na_2O \cdot 2CaO \cdot 3SiO_2$ crystals occurs via nucleation of a solid solution that is strongly enriched in sodium, and whose average composition varies during growth approaching the stoichiometric one with an increase of the crystal size. Thus, in order to discuss theoretically the values of $t^g_{ind}$ and $t^n_{ind}$ we have to take into account this crystallization path.

In the present work, to estimate the evolution of the average composition of the crystalline phase we employed the temperature of reversible polymorphic transition, $T_{pm}$, measured by DSC, which strongly depends on crystal composition, as shown in Fig. 10. By plotting $T_{pm}$ versus volume fraction crystallized, $f$, we estimated the time-dependence of the average content of sodium oxide in the solid solution using the $f(t)$-plot and employing the $T_{pm}(C_{Na_2O})$-graph as the standard, Fig. 10. The extrapolation of the $T_{pm} \sim f$ dependence to $f = 0$ allows one to estimate the composition of the critical nuclei, which is quite close to that estimated in [3] via EDS, see Fig. 11.

Figs. 12 and 13 show the time evolution of the average composition of the crystals and the size of the largest crystals at $T = 580$ °C and 590 °C, respectively. The dependence of $a(t)$ on time $t$ at a moderately advanced stage of phase transformation begins to deviate from linearity due to the difference in the compositions of the crystals and the vitreous matrix. This and other relevant effects were discussed in detail in Ref. [18]. In connection with the consid-

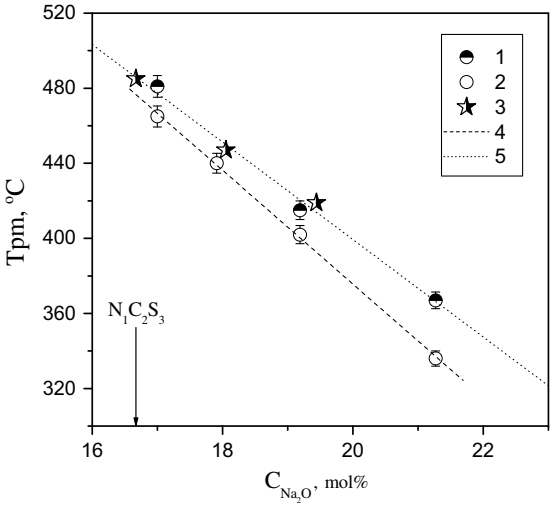


**Fig. 10.** Temperature of the reversible polymorphic transition from heating (1, 3) and cooling (2) DSC-curves versus sodium oxide content in glasses of composition belonging to metasilicate section $CaO \cdot SiO_2$-$Na_2O \cdot SiO_2$ (3) data from [21]. Lines (4) and (5) are linear fits.

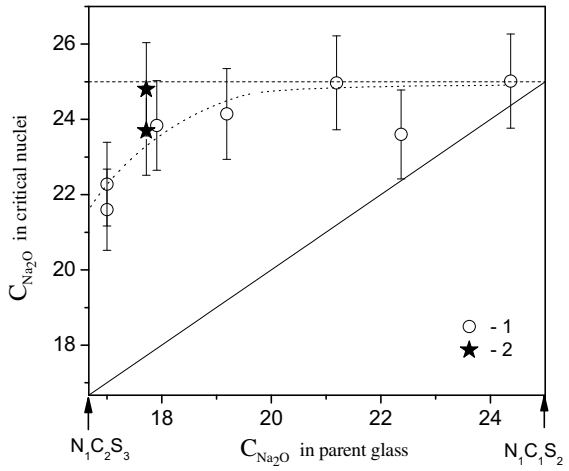


**Fig. 11.** Composition of critical nuclei estimated by extrapolation of EDS (1) [3] and $T_{pm}$ (2) data versus composition of parent glass. Solid line shows the composition of critical nuclei if it was equal to that of the glass.

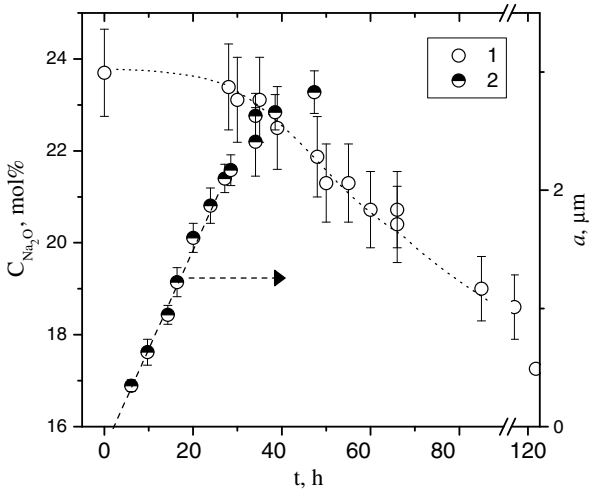


**Fig. 12.** Average crystal composition (1) and largest crystals size (2) versus time of heat treatment at $T = 580$ °C. The dashed line is linear fit of the initial part of the $a \sim t$ plot. The dotted line is just to guide the eyes.

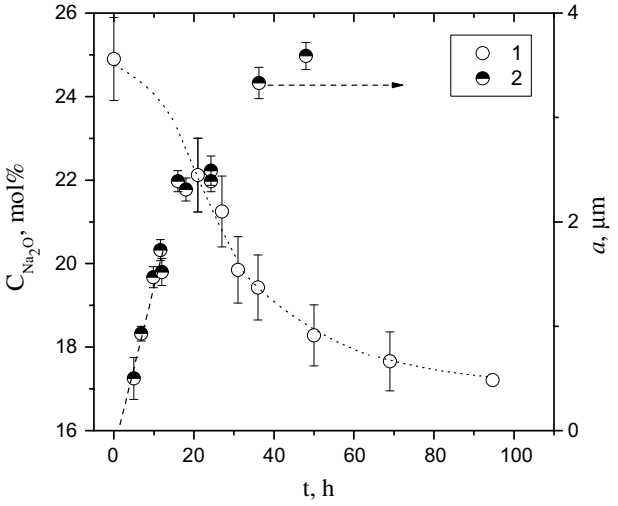


**Fig. 13.** Average crystal composition (1) and largest crystals size (2) versus time of heat treatment at $T = 590$ °C. The dashed line is a linear fit of the initial part of the $a \sim t$ plot. The dotted line is just to guide the eyes.

ered problem, it is important to note that, in order to estimate $t^g_{ind}$, the linear part of the $a(t)$-plot was used. According to Figs. 12 and 13, the average composition of the growing solid solution crystals in this period of time is closer to that of the near-critical nuclei than to the final stable phase. This fact implies that growth kinetics employed to estimate $t^g_{ind}$ and the corresponding nucleation kinetics refer to the same or to a very similar phase, which differs from the stable phase $N_1C_2S_3$. This result provides an explanation for the similarity of $t^n_{ind}$ and $t^g_{ind}$. Since the selection of the linear part of the $a(t)$-plot is rather subjective and the number of experimental points in this region is not large, the fitting procedure to Eqs. (13) and (14) is difficult to perform. Nevertheless, the time-lag estimated from growth kinetics is somewhat smaller than that estimated from the $N(t)$-plot for nucleation. To employ Eqs. (13) and (14) we assume kinetically limited growth not only of the near-critical clusters, but also of the macroscopic crystals in the initial stage, based on the linear $a(t)$-dependence. That is, we suppose that the effective diffusion coefficient is high enough and growth is only limited by interfacial diffusion processes. A better result was obtained by employing Eq. (14), see Fig. 14. Here it should be noted again that a reduction of $\tau_{C\&K}$ due to the effect of

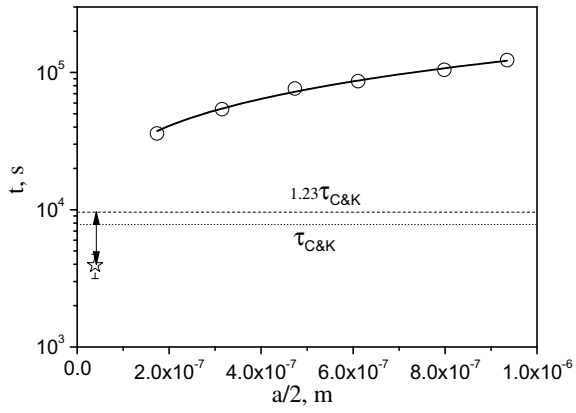


**Fig. 14.** Time $t$, needed to arrive at crystal size $a/2$ in glass $N_1C_2S_3$ at $T = 580$ °C. The circles refer to experimental data. The solid line was plotted by Eqs. (14) using $\tau_S$ and $a_*/2$ as fit parameters. The coordinates of the star show these parameters. The dotted and dashed lines show the value of $\tau_{C\&K}$ (estimated by fit of the $N(t)$-data to Eq. (2)), and $1.23\tau_{C\&K}$, respectively.

dissolution of sub-critical nuclei at the 'development' temperature [14] can diminish the difference between $\tau_S$ and $1.23\tau_{C\&K}$, contrary to the case of lithium silicate glasses.

## 6. Conclusions

For lithium silicate glasses, the time-lag for nucleation estimated from experimental crystal growth kinetics exceeds the time-lag directly estimated from nucleation kinetics by about one order of magnitude, independently on the employed solution of the Frenkel–Zeldovich equation. This discrepancy provides indirect evidence for compositional or structural deviations of the properties of the critical clusters from those of the evolving stable phase in these glasses.

In the case of a stoichiometric sodium calcium metasilicate glass, $N_1C_2S_3$, the nucleation time-lag estimated from crystal growth kinetics is only slightly shorter than the value evaluated directly from nucleation kinetics. This result reflects the fact that the macrocrystals used to measure crystal growth-rates have a composition that is close to that of the critical nuclei.

The results obtained for these particular glasses corroborate our opinion that, in the general case, the bulk properties of critical nuclei differ from those of the stable macroscopic phase. Moreover, it is demonstrated that important insights into the nucleation process can be gained by suitable analyzes of crystal growth kinetics. This strategy of combining analyzes of nucleation and growth in the same temperature range should be further explored for other glass-forming systems.

## Acknowledgements

Financial support by Fapesp, Capes and CNPq (Brazil) is fully appreciated by V.M. Fokin, Aluisio Cabral and E.D. Zanotto; while J.W.P. Schmelzer acknowledges the financial support by the Deutsche Forschungsgemeinschaft (DFG, Germany).

## References

[1] I. Gutzow, J. Schmelzer, The Vitreous State: Thermodynamics, Structure, Rheology and Crystallization, Springer, Berlin, 1995.
[2] E.D. Zanotto, V.M. Fokin, Phil. Trans. Royal Soc. Lond. A 361 (2002) 591.
[3] V.M. Fokin, E.D. Zanotto, N.S. Yuritsyn, J.W.P. Schmelzer, J. Non-Cryst. Solids 352 (2006) 2681.
[4] J. Deubener, R. Brückner, M. Sternitzke, J. Non-Cryst. Solids 163 (1993) 1.
[5] I. Gutzow, Contemp. Phys. 21 (1980) 121, 243.
[6] E.D. Zanotto, M.L. Leite, J. Non-Cryst. Solids 202 (1996) 145.
[7] F.C. Collins, Z. Electrochem. 59 (1955) 404.
[8] D. Kashchiev, Surface Sci. 14 (1969) 209.
[9] V.A. Shneidman, Sov. Phys.-Tech. Phys. 57 (1987) 131.
[10] V.A. Shneidman, Sov. Phys.-Tech. Phys. 58 (1988) 2202.
[11] V.V. Slezov, J.W.P. Schmelzer, in: J.W.P. Schmelzer, G. Röpke, V.B. Priezzhev (Eds.), Nucleation Theory and Applications, Joint Institute for Nuclear Research Publishing, Dubna, Russia, 1999.
[12] V.V. Slezov, J.W.P. Schmelzer, Phys. Rev. E 65 (2002) 031506.
[13] J. Deubener, M.C. Weinberg, J. Non-Cryst. Solids 231 (1998) 143.
[14] V.M. Fokin, E.D. Zanotto, J.W.P. Schmelzer, J. Non-Cryst. Solids 278 (2000) 24.
[15] O.V. Potapov, PhD thesis, Grebenshchikov Institute for Silicate Chemistry, Russian Academy of Sciences, Saint Petersburg, Russia, 2002.
[16] C.J.R. Gonzalez-Oliver, PhD thesis, University of Sheffield, Great Britain, 1979.
[17] V.V. Slezov, J.W.P. Schmelzer, A.S. Abyzov, in: J.W.P. Schmelzer (Ed.), Nucleation Theory and Applications, WILEY-VCH, Berlin-Weinheim, 2005, p. 39.
[18] J.W.P. Schmelzer, A.R. Gokhman, V.M. Fokin, J. Colloid Interf. Sci. 272 (2004) 109.
[19] V.M. Fokin, J.W.P. Schmelzer, M.L.F. Nascimento, E.D. Zanotto, J. Chem. Phys. 126 (2007) 234507.
[20] D. Tatchev, G. Goerigk, E. Valova, J. Dille, R. Kranold, S. Armyanov, J.-L. Delplancke, Appl. Crystallogr. 38 (2005) 787.
[21] I. Maki, T. Sugimura, J. Ceram. Assoc. Jpn. 76 (1968) 144.
[22] V.M. Fokin, O.V. Potapov, E.D. Zanotto, F.M. Spianderelo, V.L. Ugolkov, B.Z. Pevzner, J. Non-Cryst. Solids 331 (2003) 240.